

01 Jan 2007

# Frequency-Domain Measurement Method for the Analysis of ESD Generators and Coupling

Jayong Koo

Qing Cai

Giorgi Muchaidze

Andrew Martwick

*et. al. For a complete list of authors, see https://scholarsmine.mst.edu/ele_comeng_facwork/677*



## Recommended Citation

J. Koo et al., "Frequency-Domain Measurement Method for the Analysis of ESD Generators and Coupling," *IEEE Transactions on Electromagnetic Compatibility*, Institute of Electrical and Electronics Engineers (IEEE), Jan 2007.

The definitive version is available at https://doi.org/10.1109/TEMC.2007.902190

# Frequency-Domain Measurement Method for the Analysis of ESD Generators and Coupling

Jayong Koo, Qing Cai, Giorgi Muchaidze, Andy Martwick, Kai Wang, and David Pommerenke, *Senior Member, IEEE*

***Abstract*—A method for analyzing electrostatic discharge (ESD) generators and coupling to equipment under test in the frequency domain is proposed. In ESD generators, the pulses are excited by the voltage collapse across relay contacts. The voltage collapse is replaced by one port of a vector network analyer (VNA). All the discrete and structural elements that form the ESD current pulse and the transient fields are excited by the VNA as if they were excited by the voltage collapse. In such a way, the method allows analyzing the current and field-driven linear coupling without having to discharge an ESD generator, eliminating the risk to the circuit and allowing the use of the wider dynamic range of a network analyzer relative to a real-time oscilloscope. The method is applicable to other voltage-collapse-driven tests, such as electrical fast transient, ultrawideband susceptibility testing but requires a linear coupling path.**

***Index Terms*—Electrostatic discharge (ESD), network analyzer (NWA), simulation.**

## I. Introduction

ELECTROSTATIC discharge (ESD) is reproduced by an ESD generator to test the robustness of various electronics devices toward ESD. Most ESD generators are built in accordance with the specifications given in IEC 6100-4-2 [1]. The discharges are initiated by high-voltage relays. While the mechanical movement is slow, the electrical breakdown leads to subnanosecond voltage changes. Before the contacts touch, a surface-driven or gas-discharge-driven (depending on the voltage) breakdown will lead to a rapid voltage collapse. These fall times have been estimated to be less than 100 ps [2]. However, the discharge current specifications call for 700–1000 ps rise time. This is achieved by pulse forming elements placed around the relay, and between the relay and the tip of the ESD generator. Not only the injected ESD current, but also the rapidly changing currents within the relay and in the pulse-forming elements cause transient fields. As shown in [2] and [3], this may lead to excessive $>1$ GHz transient fields of ESD generators compared to human-metal ESD of equivalent current rise time.

Compliance of electronic equipment is determined by the reaction against disturbance as indicated in the regulation [1].

However, such tests reveal little information on the underlying reason for a disturbance, such as the coupling paths. Knowing the coupling paths cannot only help resolve ESD issues, but can also be used to estimate system performance beforehand.

Several numerical and circuit models of ESD generators have been published and verified by measurement [4]–[6]. For analyzing $>1$ GHz frequency components, it is not sufficient to take a discharge current of 0.7–1 ns rise time as the excitation source. The details of the pulse-forming network also need to be modeled to correctly reproduce the $>1$ GHz field components. Thus, not only a detailed model of the electronic system to which the discharge will be applied is needed, but it must also be combined with a rather elaborate ESD generator model.

Numerous authors have applied numerical methods for calculating coupling of transient fields from ESD [7]–[11]. However, compared to practical systems, the authors used relatively simple structures as most real systems are too complex to be modeled by numerical means.

This drawback can be avoided by experimental methods [10]–[13]. These methods have a common feature that ESD generators are discharged while induced voltages or currents are measured. However, the following set of difficulties arise.

- The strong common-mode coupling to the probing system may override the intended signal.
- Dynamic ranges of fast time-domain oscilloscopes are limited by eight-bit A/D converters.
- The high voltages endanger the device under test, the active test probes, and possibly the oscilloscope.

In most cases, the dominated coupling path involves metal shielding and coupling to wires and traces. If we limit our analysis to such linear coupling paths, then frequency-domain methods can be used.

Using the frequency domain for such coupling analysis offers several significant advantages. The wider dynamic range and high accuracy of the vector network analyer (VNA) can be utilized together with the, usually built-in, time-domain transformation functions. Further, it avoids endangering the device under test or the test equipment.

This paper describes a frequency-domain method for conducting coupling studies associated with ESD generator or other voltage-collapse-driven susceptibility problems. The novelty lies in correctly representing the currents and transient fields of all structural and discrete elements of the pulse-forming circuit within the ESD generator.

Section II introduces the methodology, Section III presents the currents and field-measurement results in comparison to nonmodified ESD generators, Section IV discusses the applications and limitations of the method, and Section V presents the conclusions.

Manuscript received September 13, 2006; revised February 8, 2007.

J. Koo, Q. Cai, G. Muchaidze, and D. Pommerenke are with the Electromagnetic Compatibility Group, University of Missouri-Rolla, Rolla, MO 65409 USA (e-mail: jkhy6@umr.edu; qcync@umr.edu; gmfh3@umr.edu; davidjp@umr.edu).

A. Martwick and K. Wang are with Intel Corporation, Hillsboro, OR 97124 USA (e-mail: andy.martwick@intel.com; kai.a.wang@intel.com).

Digital Object Identifier 10.1109/TEMC.2007.902190

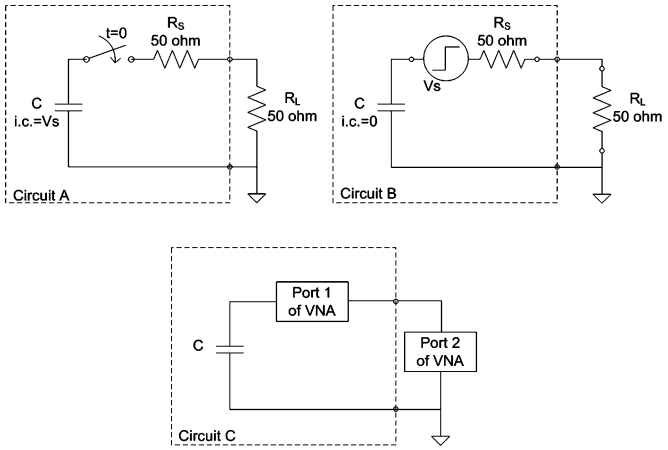


Fig. 1. Three different circuits that express the simple capacitor discharge current flowing through the resistor $R_L$.

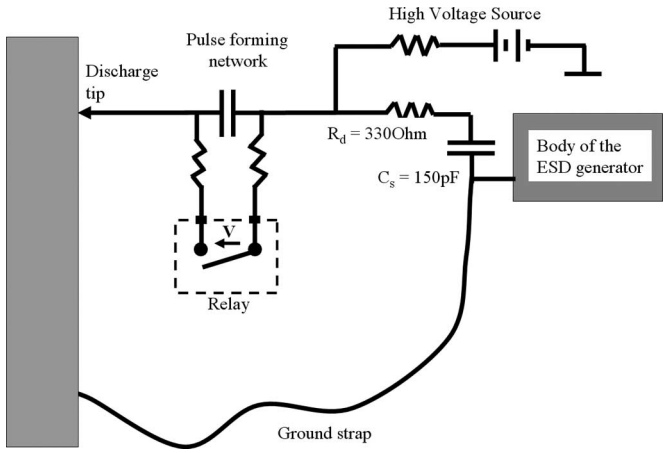


Fig. 2. Simple equivalent circuit of an ESD generator. The high-voltage source charges up the energy storage capacitor ($C_s$). The capacitor starts to discharge the moment the relay is closed.

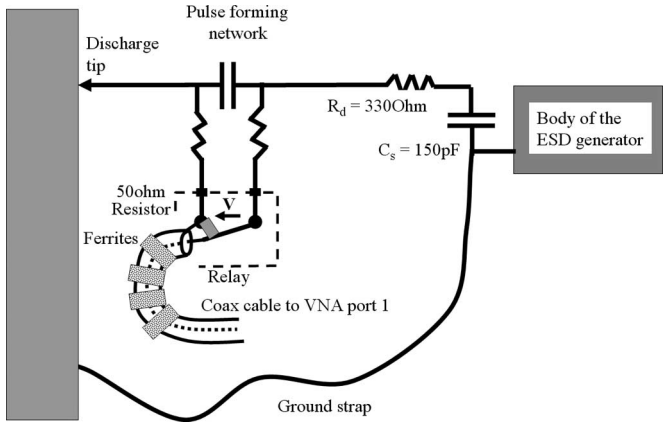


Fig. 3. Simple equivalent circuit of a modified ESD generator. In order to emulate the time-domain behavior of the circuit, the voltage collapse is substituted by the VNA port 1 to allow direct contact to the relay blades. The relay enclosure was opened.

## II. Methodology

### A. Basic Concept

The method is based on the similarity of time and frequency domains for linear systems. To illustrate the principle, let us start by using three circuits that represent a highly simplified ESD generator discharging into a load.

In Fig. 1, Circuit A, a capacitor $C$, having an initial voltage $V_s$, is discharged by an ideal relay at $t = 0$. Current flows through $R_S$ and $R_L$. Our interest is the voltage across $R_L$. The circuit elements $C$, $R_s$, and the switch act as a highly simplified ESD generator and the resistor $R_L$ as the equipment under test (EUT).

Analyzing the voltage and currents at the terminals connecting to $R_L$ for $t > 0$, there is no difference between a capacitor having an initial voltage $V_s$ in series with a switch (Circuit A) relative to a capacitor without initial voltage in series with a step function voltage source (Circuit B).

In practice, one could substitute the relay by the step function port of a time domain transmission (TDT) instrument and measure the voltage across $R_L$ (the coupled voltage) at the oscilloscope port. However, the dynamic range of TDT instruments is much less than the dynamic range of network analyzers (NWAs), and TDT sampling heads can easily be damaged by accidental ESD. Consequently, we substitute a NWA for the TDT instrument. The implementation of the principle is shown in Fig. 1, Circuit C.

Port 1 is connected in place of the relay, while port 2 measures the voltage across the 50-Ω resistor. The internal time-domain transformation of the NWA is used to obtain the time-domain results. The dynamic range of a NWA is typically better than 100 dB compared to 50–60 dB for a TDT measurement and about 40 dB for a real-time oscilloscope measurement if no averaging or other signal-enhancing techniques are applied.

### B. Implementation

The main building blocks of an ESD generator are a high-voltage source, a relay, a pulse-forming network, a discharge resistor ($R_d$), an energy storage capacitor ($C_s$), a ground strap, and the body of ESD generator (see Fig. 2). The high-voltage source charges up $C_s$, while the relay is open. The moment the gap between the relay blades is small enough, a breakdown will cause the capacitor to discharge.

As the excitation of this circuit occurs at the relay blade contact, port 1 of the NWA needs to be connected at the blades as shown in Fig. 3. Obviously, the high-voltage source needs to be turned off, if not removed. The NWA excites the ESD generator circuit by its internal source.

The voltage $V$ in Fig. 2 collapses very rapidly [5]. It approximates a step-response excitation to the ESD generator. Using the chirp-Z inverse Fourier transform and windowing function built in the VNA, this step response can be readily displayed based on the S21 data.

The discrete Fourier transform (DFT) is expressed as

$$X_k = X(z_k) = \sum_{n=0}^{N-1} x_n z_k^{-n}, \qquad k = 0, 1, \ldots, N-1 \quad (1)$$

where $z_k = \exp(j2\pi k/N)$.

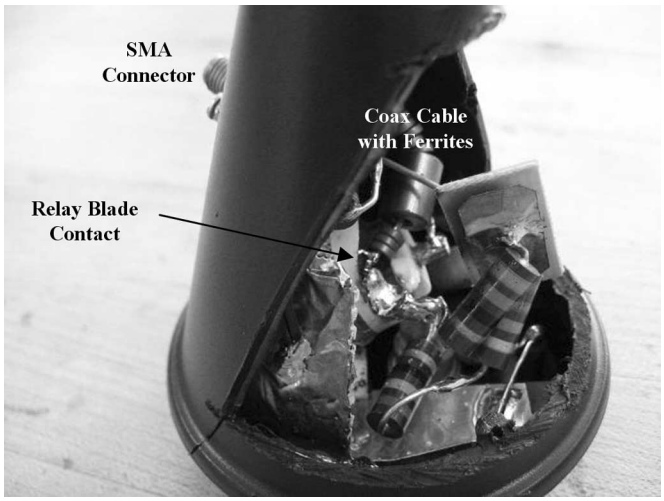


Fig. 4. Modified ESD generator module. The relay was opened and the coaxial cable was soldered to the relay blade contacts. The SMA connector connects to the NWA.

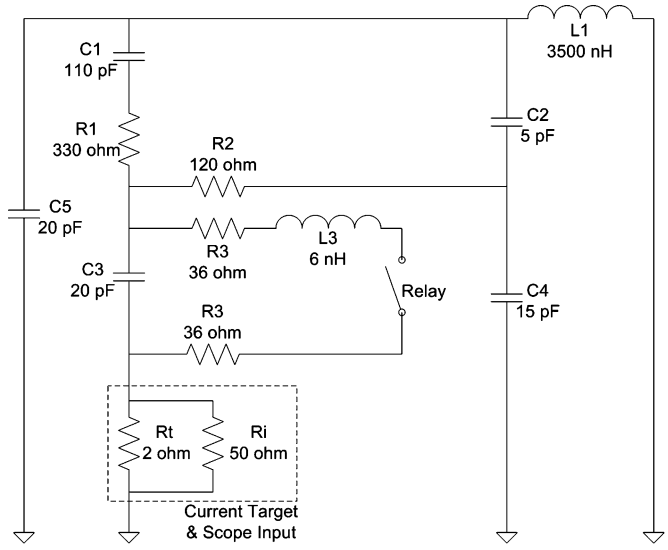


Fig. 5. Equivalent circuit of a ESD generator. $R_t$ and $R_i$ represent the current target resistance and input impedance of the oscilloscope.

If we have $z_k$ in the following form, it is called the chip-Z transformation (CZT):

$$z_k = AW^{-k}, \qquad k = 0, 1, \ldots, M-1 \tag{2}$$

where $M$ is an arbitrary integer, and both $A$ and $W$ are arbitrary complex numbers of the form $A = A_0 e^{j2\pi\theta_0}$ and $W = W_0 e^{j2\pi\phi_0}$.

The case $A = 1, M = N$, and $W = \exp(-j2\pi/N)$ corresponds to the DFT.

The CZT is one of the computational algorithms of sampled $z$-transform, which is more general and flexible than the fast Fourier transform (FFT) in their applications [16].

Windowing is needed because the band-limiting response of a frequency-domain measurement causes ringing in the time-domain response. Windowing improves the dynamic range of the time-domain results by filtering the frequency-domain data prior to converting it to the time domain, at the expense of the fine frequency resolution of the transformed data [17], [18].

Port 2 of the VNA can be connected to various types of transducers, e.g., the output of an ESD current target to capture the ESD discharge waveform, the output of a current clamp to measure the currents induced in wires internal to an electronic system, to field sensors, or to traces on a printed circuit board. Such results are presented in Section III.

The underlying methodology, as outlined above, is quite simple. However, to achieve good results, a careful implementation is needed. Three points need special attention.

1) Port 1 of the VNA needs to be connected exactly across the relay blades at the point of contact. Any deviation from this will change the RF behavior because the point of excitation would be moved away from its correct location. The ceramic enclosure of the relay was opened to allow direct contact to the relay blades by a thin coaxial cable (see Fig. 4).
2) The source impedance should match the impedance created by the spark within the relay of the ESD generator circuit. The impedance across the contacts evolves through three phases. At first, it is an open circuit ($t < 0$); next, the relay is best described by a time-varying resistance ($t = 0$ to about 100 ps); then, the relay is best described by a series voltage source of 25–40 V. Replacing the relay with a 50-$\Omega$ VNA port leads to additional losses and damping of ringing by the pulse-forming circuit (see Section IV). A 39-$\Omega$ SMD resistor was soldered parallel to the relay contacts to reduce the source impedance. This resister is shown in Fig. 4.
3) The attached cable needs to be electromagnetically invisible, i.e., no common-mode current is allowed to flow on it. A combination of low-frequency and high-frequency (brand name "Gigabuster") material has been used to reduce the common-mode currents. The exact arrangement is the result of experimental optimization.

### C. Verification of the Methodology by SPICE Simulation

A SPICE simulation was used to verify the proposed method. Based on the equivalent circuit of an ESD generator given in [5], the modifications needed for the frequency-domain method have been implemented.

Several types of the equivalent circuits for ESD generators have been proposed [4]–[6]. For the circuit shown in Fig. 5, the resistors $R_t$ and $R_i$ represent the current target resistance and input resistance of the oscilloscope, respectively. The function of each component is explained in [5, Table I]. The capacitor $C$ 1 is charged to an initial value. This represents the charging by the high-voltage source of an actual ESD generator. After closing the relay, the discharge current flowing through $R_t$ is probed.

The modified generator is shown in Fig. 6.

1) The step voltage source $V_s$ represents the swept frequency source of the NWA.
2) The inductance of the ground strap is represented by $L$ 1. The electric near-field coupling within the ESD generator

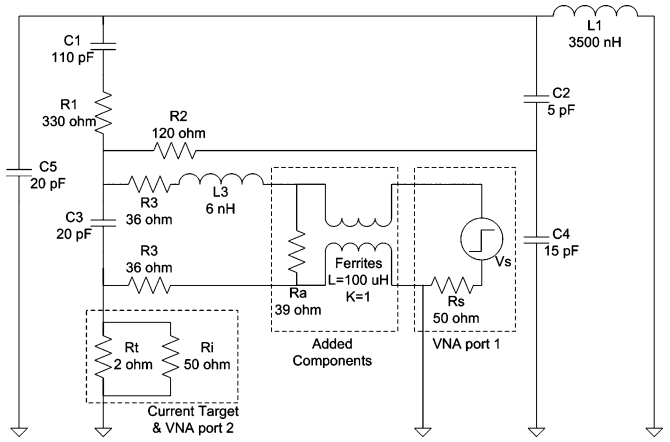


Fig. 6. Equivalent circuits of the modified ESD generator. Resistors $R_t$ and $R_i$ represent the current target resistance and input impedance of the VNA port 2. Port 1 is represented by a voltage source $V_s$, and the internal impedance $R_s$. The transformer and $R_a$ indicate the ferrites and the added resistor for reducing source impedance, respectively.

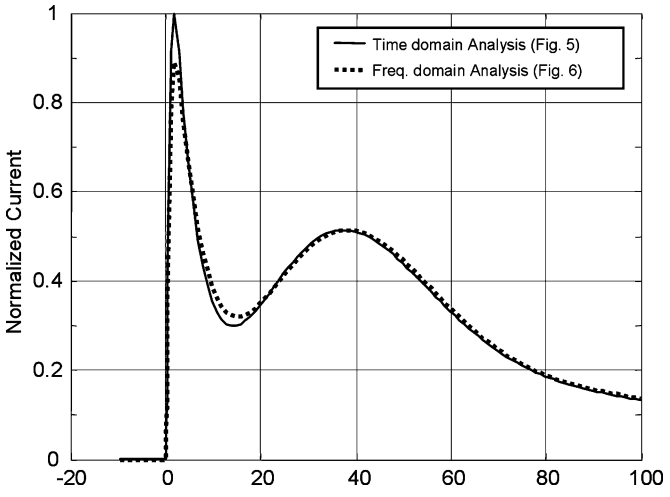


Fig. 7. Comparison of computed currents using time-domain (Fig. 5) and the frequency-domain analysis (Fig. 6).

is modeled as capacitor. No radiation effects are taken into account.

3) Ferrites are modeled as pure common-mode inductors. Port 2 of the VNA is connected across the current target resistor $R_t$. Port 1 is connected to the relay contacts. The ferrites are modeled as a transformer, which has two perfectly coupled inductors whose values are 100 uH each. $R_a$ is to reduce the source impedance of port 1.
4) The circuit shown in Fig. 6 allows two paths to ground: one via the ground strap and one via the NWA. This may change the late time part of the current waveform. To avoid this effect, low-frequency high-permeability ferrites (in conjunction with high-frequency ferrites) were placed around the coaxial cables. The combined effect is modeled by the two perfectly coupled inductors.

The current waveforms calculated using the circuits shown in Figs. 5 and 6 are compared in Fig. 7. The data are scaled such that the second peaks have the same magnitude. Both waveforms are similar; however, the circuit shown in Fig. 6 yields a reduced

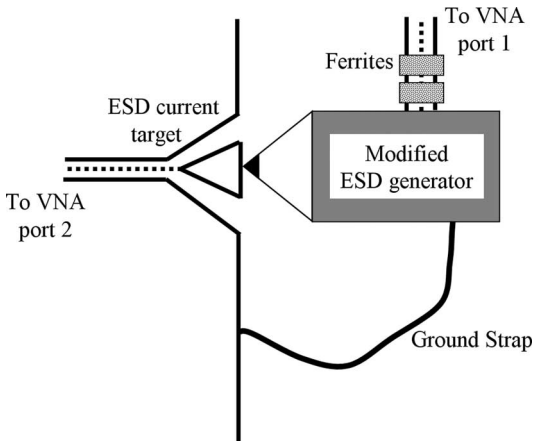


Fig. 8. Frequency-domain measurement setup using VNA for the discharge current waveform.

first peak value, less swing, and a larger rise time. This is a result of the source impedance given by the parallel connection of $R_s$ and $R_a$. The source impedance increases the time constant of the pulse-forming resistor-capacitor-resistor (RCR) filter, leading to a slightly slower rise time and a decreased discharge current.

## III. Measurement Results

In each data set, a time-domain measurement (standard ESD generator) is compared to a frequency-domain measurement using the modified ESD generator. Three such pairs are presented, each emphasizing different aspects of ESD testing.

### *A. Time-Domain and Frequency-Domain Instrumentation*

The testing used a 1-kV setting of the normal ESD generator and a Tektronix 7404 (4 GHz BW, 20 GS/s) oscilloscope. The oscilloscope was connected to the output of an ESD current target, an F-2000 current clamp or a small loop, respectively. For the frequency-domain measurements, an HP8753 D VNA was used.

To compare the discharge current waveform, a current target was selected as the verification method. This is the best controlled measurement on ESD generators possible (see Fig. 8). The current target was mounted on the side wall of a shielded room. The second set of verification measurements used a small loop. Due to the derivative relationship between the field and the induced voltage, this setup emphasized the high-frequency components of the fields.

In the third set of tests, a structure was selected that reflected the intended application of the method, i.e., the measurement of the coupling to the wires connecting to a personal computer (PC) mother board. More details of the measurement setup are shown in Fig. 13.

Fig. 9 compares the time- and frequency-domain measurements. The VNA measurement matches the general shape quite well; however, some deviations in the fine structure show up. The oscillations are more attenuated if they are captured using the VNA. Most likely, this is a result of the source impedance of the VNA (39 $\Omega \| 50\ \Omega$) and the loading of the relay by the

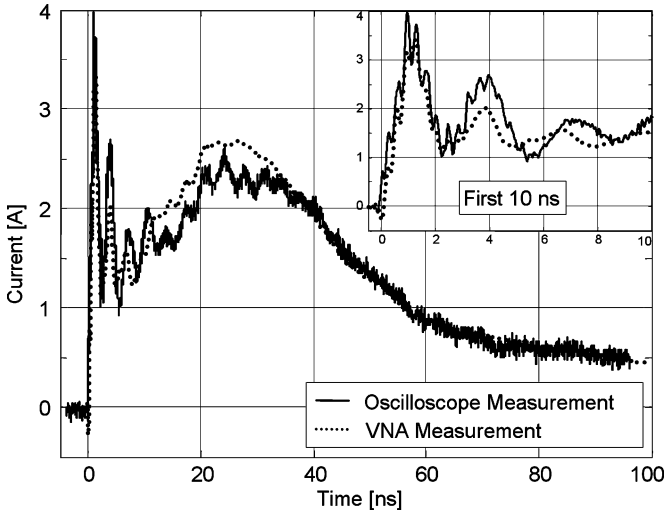


Fig. 9. ESD discharge current measured using the oscilloscope (Tektronix 7404, 4 GHz BW, 20 GS/s) compared to VNA measurements (HP8753D).

common-mode impedance of the strongly ferrite loaded coaxial cable. The SPICE simulation of Section II shows effects such as shifts in the frequency of the oscillations and larger attenuation.

We do not consider these differences to limit the range of applications of this method, given the variations seen between different samples of the same ESD generator models and especially between different brand simulators.

### *B. Induced Loop Voltage Measurement in Frequency Domain*

In [2], it has been shown that the transient fields are not only caused by the current at the injection point, but also by the currents within the inner structure of the ESD generator. Due to the difference in current rise times, the >1 GHz fields will be dominated by currents of the inner structure. To see the validity of the frequency-domain analysis for fields especially at higher frequencies, the voltage induced in a small loop has been measured.

A semicircular loop (28-mm diameter, 0.7-mm wire diameter) was placed on a ground plane and connected to the oscilloscope or VNA, respectively. See Fig. 10 for the test setup and Figs. 11 and 12 for the results. These results indicate that the VNA method of measurement correctly excites the high-frequency currents within the ESD generator.

### *C. Measurements of the Voltage Induced on a Trace on a Mother Board in the Frequency Domain*

A third test setup was selected that reflects the ESD coupling into the wiring and trace connected to an IC on a PC mother board. The other two test setups only emphasize one coupling path. The current target is useful for verifying if the discharge current is reproduced well, and a small loop is used mainly to capture the transient fields and emphasizes the high-frequency fields due to the derivative nature of the coupling.

Prior to measuring the voltage on the trace, the mother board was analyzed using the methods outlined in [14] and [15]. This showed that the "Power Good" trace was the most sensitive to

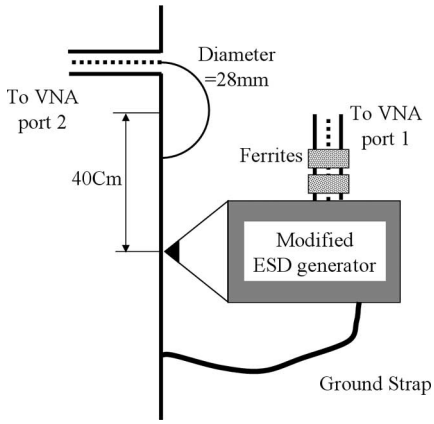


Fig. 10. Frequency-domain measurement setup using a VNA for induced loop voltage measurement.

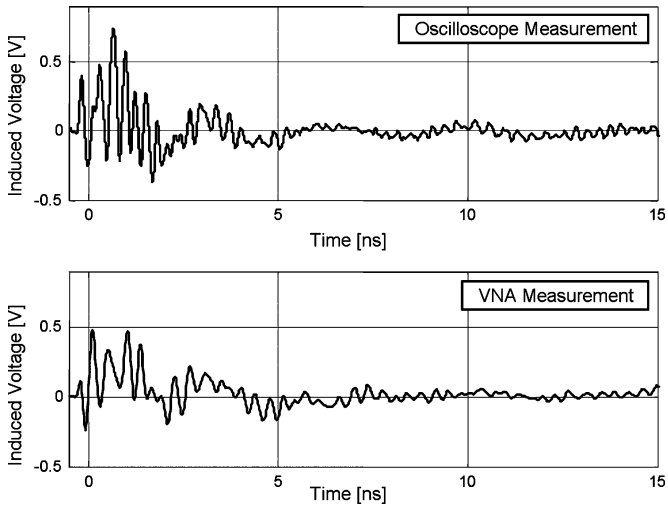


Fig. 11. Induced loop voltage for the measurement shown in Fig. 10.

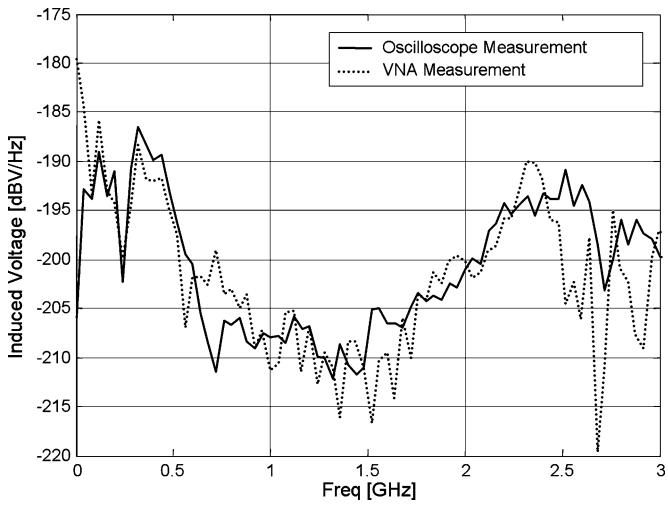


Fig. 12. Spectrum of the induced loop voltage for the measurement shown in Fig. 10.

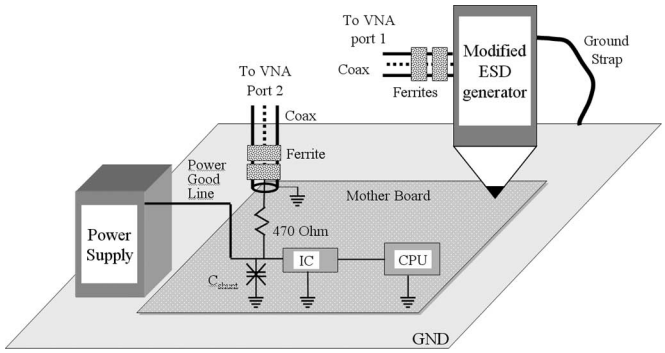


Fig. 13. Measurement setup for the ESD coupling to the mother board connecting wire and trace.

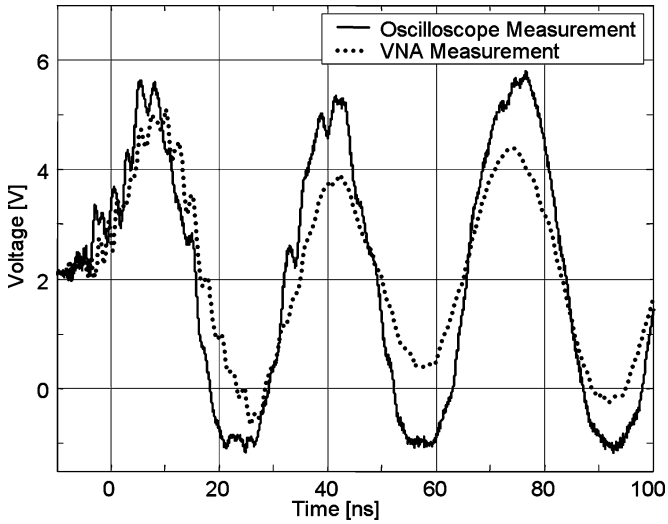


Fig. 14. Disturbed voltage measured on the "Power Good" trace on the computer mother board. The ESD generator was charged to $-0.5$ kV. The frequency-domain data were shifted by 2 V dc.

ESD. For this reason, it was selected for monitoring the voltage induced by ESD.

The measurement setup is shown in Fig. 13. The operating mother board was placed on a metal plane using an insulating spacer. The ESDs from the generator were applied on the ground of the mother board while the voltage on the trace was measured. A ferrite-loaded coaxial cable and a 470-$\Omega$ SMT resistor were used to probe the voltage on the trace. A shunt capacitor $C_{\rm shunt}$ that filters the "Power Good" line coming from the power supply was removed to ensure that the upset of the mother board will be caused by coupling into the "Power Good" line (PGL) wiring. This dropped the level at which the board resets from 8 to about 4 kV.

In Fig. 14, the comparison between the time-domain and the frequency-domain measurements are shown. The ESD generator was charged to $-0.5$ kV. At that level, the mother board acts linearly; thus, the trace voltage can be reproduced by the suggested method.

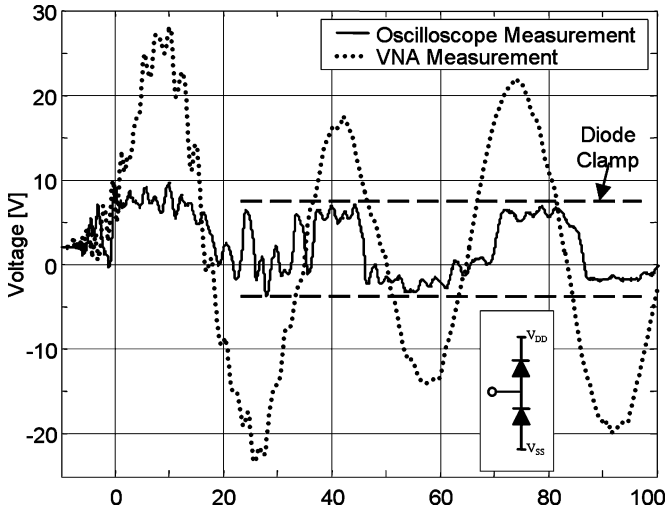


Fig. 15. Disturbed voltage measured on the "Power Good" trace on the computer mother board. The ESD generator was charged to $-4.5$ kV, and the clamping effect is shown.

## IV. Discussion—Limitations of the Method

The test data indicate that the VNA method is able to reproduce the ESD generator up to about 2 GHz. But the following limitations need to be considered for the proper application of the method.

### *A. Linearity*

It requires that the coupling path is linear with respect to the applied discharge voltage. ESD generators used in contact mode are linear with respect to the charge voltage, i.e., the current waveform scales with voltage. Most coupling paths are formed by passive elements, e.g., shields, traces, and inductive or capacitive coupling. In these cases, the proposed methodology would correctly determine the currents and voltages on the traces. However, if clamping effects of the ICs or nonlinear ESD protection is determining the voltages, the method could only be applied if the linear effects of "coupling into a trace" can be separated from the nonlinear effect of voltage clamping.

Fig. 15 shows an example of clamping. The measurement set up was the same as the one for Fig. 14, but the ESD generator was charged to $-4.5$ kV. The frequency-domain data were scaled with the discharge voltage. If there is no dominate nonlinear effect, the coupled voltage should scale linearly with the charge voltage of the ESD generator. However, at $-4.5$ kV, we see the clamping of the input voltage of the IC caused by the ESD protection diodes. Such clamping cannot be simulated by the VNA method suggested.

When soft-errors are caused by ESD, the induced voltages are often below the clamping thresholds, as bit-flipping can occur at voltage levels between ground (GND) voltage and voltage drain drain (VDD). Of course, in cases in which a primary ESD causes a secondary breakdown, the methodology will not be able to reproduce the coupled voltages. Overall, we suggest using the method for coupling measurements, but not for circuit-response

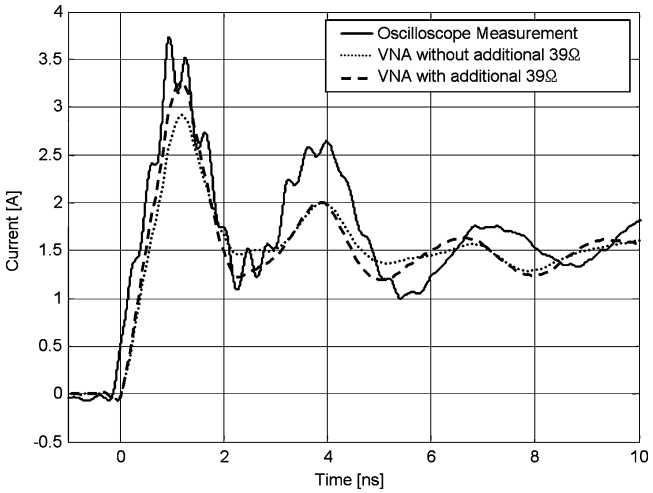


Fig. 16. Frequency-domain measurement data with and without an additional parallel 50-Ω resistor are shown together. The effect of source impedance modeling for the voltage collapse between the relay contacts can be seen.

measurements. It offers the opportunity of ESD analysis without the risk of damage, as one may want to perform in complex one-of-the kind systems. Those would need to be modeled, e.g., using SPICE by combining the coupling data with the nonlinear circuits.

### *B. Equality of the Excitation*

The relay blade contact is substituted by a 50-Ω VNA port having an additional 39-Ω resistor in parallel. However, the impedance of the spark within the relay cannot simply be represented by a 22 Ω (50 Ω paralleled by 39 Ω). If sufficient current is flowing, it is better modeled by a constant 25–40 V drop than by a resistor. The effect of the source impedance has been analyzed by comparing two cases: a 50-Ω source impedance and a 22-Ω source impedance. It can be seen in Fig. 16 that the higher impedance leads to less ringing, indicating that even 22 Ω might not be sufficiently low to fully represent the details of the initial peak of the waveform. However, since the objective is to determine the coupling, one needs to weigh the differences in the waveforms against the variability of the coupling. Its variability is determined by the reproducibility of the chassis contacts and the wire positions.

### *C. Common-Mode Currents Flowing on the Coaxial Cable*

Ideally, the excitation would not alter any currents within the ESD generator and its ground strap. However, an additional cable is attached. Common-mode currents on this cable alter the current and radiation characteristics. In our experiments, a 20-mil semirigid cable, having many ferrite sleeves along its length and additional high permeability material to suppress any low-frequency currents, was used. However, the common-mode current cannot be fully suppressed. This somewhat attenuates the oscillations.

## V. Conclusion

A method for characterizing ESD generators and coupling in the frequency domain has been proposed. This method allows the analysis of both discharge current and field effects due to the high-voltage breakdown in the ESD generators without the need to operate at high voltages. The method has been substantiated by SPICE simulations and verified by comparison of modified to nonmodified ESD generators.

## References

[1] *EMC—Part 4-2: Testing and Measurement Techniques—Electrostatic Discharge Immunity Test*, IEC International Standard 61000-4-2, 2001.

[2] R. Chundru, D. Pommerenke, K. Wang, T. V. Doren, F. P. Centola, and J. S. Huang, "Characterization of human metal ESD reference discharge event and correlation of generator parameters to failure levels-part I: Reference event," *IEEE Trans. Electromagn. Compat.*, vol. 46, no. 4, pp. 498–504, Nov. 2004.

[3] K. Wang, D. Pommerenke, R. Chundru, T. V. Doren, F. P. Centola, and J. S. Huang, "Characterization of human metal ESD reference discharge event and correlation of generator parameters to failure levels-part II: Correlation of generator parameters to failure levels," *IEEE Trans. Electromagn. Compat.*, vol. 46, no. 4, pp. 505–511, Nov. 2004.

[4] H. Tanaka, O. Fujiwara, and Y. Yamanaka, "A circuit approach to simulate discharge current injected in contact with an ESD-gun," in *Proc. 3rd Int. Symp. Electromagn. Compat.* May 21–24, 2002, pp. 486–489.

[5] K. Wang, D. Pommerenke, R. Chundru, T. V. Doren, J. L. Drewniak, and A. Shashindranath, "Numerical modeling of electrostatic discharge generators," *IEEE Trans. Electromagn. Compat.*, vol. 45, no. 2, pp. 258–271, May 2003.

[6] F. Centola, D. Pommerenke, K. Wang, T. V. Doren, and S. Caniggia, "ESD excitation model for susceptibility study," in *Proc. IEEE Int. Symp. Electromagn. Compat.* Aug. 18–22, 2003, vol. 1, pp. 58–63.

[7] G. Cerri, R. De Leo, and V. M. Primiani, "ESD indirect coupling modeling," *IEEE Trans. Electromagn. Compat.*, vol. 38, no. 3, pp. 274–281, Aug. 1996.

[8] G. Cerri, R. De Leo, and V. M. Primiani, "Coupling between common mode ESD and transmission lines inside shielded enclosures," in *Proc. IEEE Int. Symp. Electromagn. Compat.*, Aug. 2001, vol. 2, pp. 1265–1268.

[9] R. De Leo, G. Cerri, and V. M. Primiani, "ESD in electronic equipment: Coupling mechanisms and compliance testing," in *Proc. IEEE Int. Symp. Ind. Electron.*, Jul. 2002, vol. 4, pp. 1382–1385.

[10] G. Caccavo, G. Cerri, V. M. Primiani, L. Pierantoni, and P. Russo, "ESD field penetration into a populated metallic enclosure a hybrid time-domain approach," *IEEE Trans. Electromagn. Compat.*, vol. 44, no. 1, pp. 243–249, Feb. 2002.

[11] Y. S. Huang and T. L. Wu, "Numerical and experimental investigation of noise coupling perturbed by ESD currents on printed circuit boards," in *Proc. IEEE Int. Symp. Electromagn. Compat.*, Aug. 2003, vol. 1, pp. 43–47.

[12] K. H. Chan, L. C. Fung, and S. W. Leung, "Experimental study of ESD effect on metallic enclosure," in *Proc. IEEE 3rd Int. Symp. Electromagn. Compat.*, May 2002, pp. 490–492.

[13] C. Bowman, A. Bogorad, P. Shih, D. Tasca, M. Shomberg, and J. Armenti, "Spacecraft-level current-injection testing to investigate discharge coupling models," *IEEE Trans. Nucl. Sci.*, vol. 36, no. 6, pt. 1–2, pp. 2033–2040, Dec. 1989.

[14] K. Wang, J. Koo, G. Muchaidze, and D. Pommerenke, "ESD susceptibility characterization of an EUT by using 3D ESD scanning system," in *Proc. IEEE Int. Symp. Electromagn. Compat.*, Aug. 2005, vol. 2, pp. 350–355.

[15] J. Koo, G. Muchaidze, and D. Pommerenke, "Finding the root cause of an ESD upset event," in *Proc. DesignCon 2006,* 12-WA2.

[16] L. Rabiner, R. Schafer, and C. Rader, "The chirp z-transfom algorithm," *IEEE Trans. Audio Electroacoust.*, vol. AU-17, no. 2, pp. 86–92, Jun. 1969.

[17] *User's Guide HP8753D Network Analyzer*, Hewlett-Packard, Part 08753-90257, Sep. 1995.

[18] *Time Domain Analysis Using a Network Analyzer*, Agilent Technologies, Application Note 1287-12, 2007.

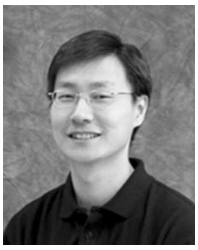

**Jayong Koo** received the B.S.E.E. degree in electrical engineering from Chung-Ang University, Seoul, Korea, in 1996 and the M.S.E.E. degree in electrical engineering from Yonsei University, Seoul, in 1998. He is currently working toward the Ph.D. degree at the Electromagnetic Compatibility Laboratory, University of Missouri-Rolla, Rolla.

He was with LG Electronics, Korea for four years and Dacom, Korea for two years. His research interests include electrostatic discharge, electromagnetic compatibility, and numerical calculation as well as advanced RF measurements.

**Qing Cai** received the B.S and M.S degrees from the Hefei University of Technology, Hefei, China, in 1999 and 2002, respectively. She is currently working toward the Master's degree in electrical engineering at the Electromagnetic Compatibility Laboratory, University of Missouri-Rolla, Rolla.

Her research interests include electrostatic discharge, electromagnetic compatibility, and advanced RF measurement.

**Giorgi Muchaidze** received the B.S.M.E. degree in mechanical engineering and the M.S.C.S. degree in computer science from Georgian Technical University, Tbilisi, in 1996 and 2002, respectively. He is currently working toward the Master's degree at the Electromagnetic Compatibility Laboratory, University of Missouri-Rolla, Rolla.

He was with the EMCoS Consulting and Software Company, Tbilisi, for three years. His research interests include system-level ESD testing and EMC/EMI measurements.

**Andrew Martwick** received the B.S. degree in physics from Excelsior University, Albany, NY, in 2007 and is currently working toward the M.S. degree at Portland State University, Portland, OR.

Since 1995, he has been with Intel Corporation, Hillsboro, OR, where he is currently an EMC Engineer. He is the holder of 29 patents in communications, computer architecture, power management, and component design. His current research interests include negative refractive materials and surface plasmons.

He is a member of the Sigma-Pi-Sigma physics honor society.

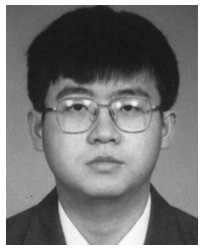

**Kai Wang** received the B.S. and M.S. degrees in electrical engineering from Tsinghua University, Beijing, China, in 1998 and 2000, respectively, and the Ph.D. degree in electrical engineering from the University of Missouri-Rolla, Rolla, in 2005.

Since 2005, he has been with Intel Corporation, Hillsboro, OR. His research interests include electromagnetic compatibility in high-speed digital and mixed-signal designs, electronic packaging, and electrostatic discharge.

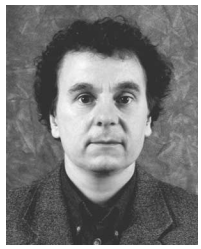

**David Pommerenke** (M'98–SM'03) received the Ph.D. degree from the Technical University of Berlin, Berlin, Germany, in 1996.

After working at Hewlett Packard for five years, he joined the Electromagnetic Compatibility Laboratory, University of Missouri-Rolla, Rolla, in 2001, where he is currently a Tenured Professor. His research interests include EMC, ESD measurement techniques, EMI analysis methods, and numerical methods and instrumentation for EMC and high voltage. He is the author of more than 100 publications and is the holder of seven patents. He is the U.S. representative of the ESD standard setting group within the IEC TC77b.